TOPOGRAPHIC ANALYSIS OF A COARSE-GRAINED RIPPLE FIELD, ALGODONES DUNES, CALIFORNIA. L.M. Berger[1], R.C. Ewing[2], M.G.A Lapôtre[3], M. Hasson[4] [1]Texas A&M University, College Station, TX (lauren.m.berger@tamu.edu) [2]Texas A&M University, College Station, TX (rce@tamu.edu) [3]Stanford University, Stanford CA (mlapotre@stanford.edu) [4] Stanford University, Stanford CA (mhasson@stanford.edu)

Introduction: Aeolian bedforms exist across the solar system including on planets (Venus, Earth, Mars), moons (Titan), and other bodies (Comet 67P, Pluto). They are primarily recognized by their distinct morphologies and field-scale patterns. Reconstructing modern and ancient environmental and climatic conditions on these worlds relies on interpreting bedform morphology and patterns [5][8]. Analyzing 2D patterns including wavelength and orientation is an established method to assess formative conditions of dunes but has not been widely used in evaluating coarse-grain ripple patterns. Further, topographic structure of fields of aeolian bedforms is a little utilized metric for evaluating formative conditions. Here we analyze the 2D and 3D parameters of a coarse-grained ripple field in the Algodones Dune Field, California as an analog to coarse-grained ripple patterns on Mars and across the solar system.

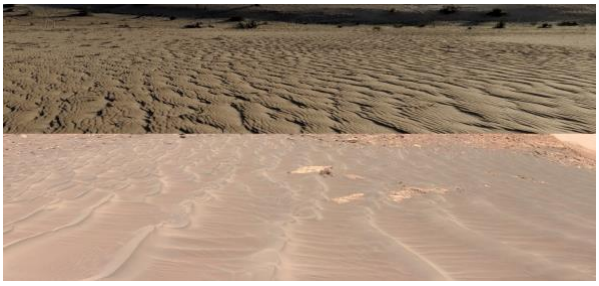

Figure 1. In Situ imagery of coarse-grained ripples at Algodones Dunes (top)(photograph by R.C. Ewing) and Gale Crater, Mars (bottom)(Curiosity MASTCAM mosaic CX01752ML0642154F553022435VA)

The Algodones Dune field (Fig. 1) possesses a wide range of aeolian bedforms across a relatively small area [3]. Compound dunes that make up the center of the dune field are flanked to the west by a deflationary sand ramp with abundant coarse-grained ripples. At Algodones Dunes, coarse-grained ripples are defined by bimodal grainsize distributions in which the coarser fraction is transported by creep and concentrates at the crest and the finer fraction is transported by saltation and concentrates on the slopes of the ripple and in the subsurface. The scale of the ripples and ripple fields make Algodones an ideal analog for in situ and orbital studies of coarse-grained ripples.

Coarse-grained ripples have been widely studied on Mars and these are the primary basis for comparison to this study. Coarse-grained ripples have been studied in situ on Mars by Curiosity [5], Spirit [11], and Opportunity [7] and identified from orbit using satellite images [Ewing et al., 2010; Silvestro et al. 2020]. Because scientists are restricted in the amount of planetary in situ data that can be collected, remote sensing to analyze terrain is a primary means of assessing large fields of aeolian bedforms. Historically, orbital data has been the primary means of analyzing bedform patterns, but the success of Ingenuity, the Mars 2020 mission helicopter, has created new opportunities to analyze bedforms from low-altitude aircraft using high-spatial resolution images.

Methods: Using a drone, high resolution optical images and a digital elevation model (1 cm/pixel) was collected to evaluate ripple morphology and patterns. The dataset's high-resolution imagery is sufficient to characterize the smallest-scale ripples (15 cm wavelength) in the field. Coarse-grained ripples were separated into stoss and lee slopes to gain a better understanding of the morphology and morphometrics of a coarse-grained ripple. The ripple slopes were mapped from the DEM using ArcGIS Pro. The slope azimuth was calculated using the aspect tool and then reclassified into eight 45° bins. Then, focal statistics calculated information about the average slope, relief, and slope azimuth values in the stoss and lee slopes.

Ripple crests were mapped south to north using ArcGIS, large wavelength ripples at a resolution of 1:20 and a representative patch of small wavelength ripples at 1:15. Mapped crests are used to calculate orientation and length averages across the field (Fig. 2 & 3).

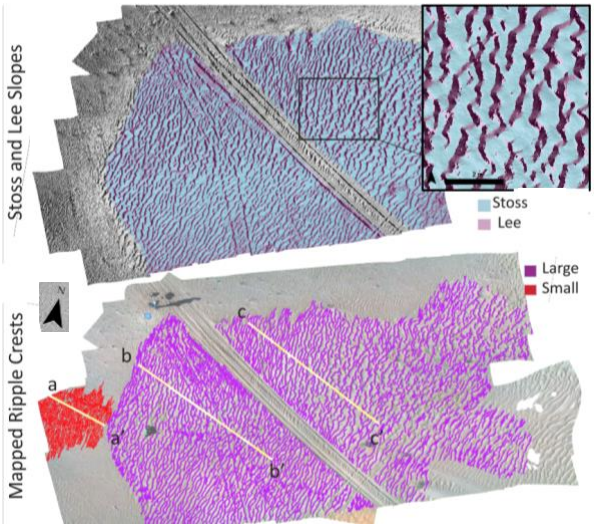

Figure 2. Top: Mapped stoss and lee slopes over a hill-shade. Bottom: Mapped large and small wavelength ripple crests.

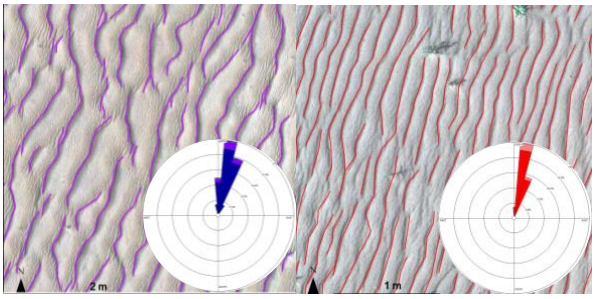

Figure 3. Zoom image of mapped ripple crests and rose diagrams for large wavelength (left) and small wavelength (right) ripples.

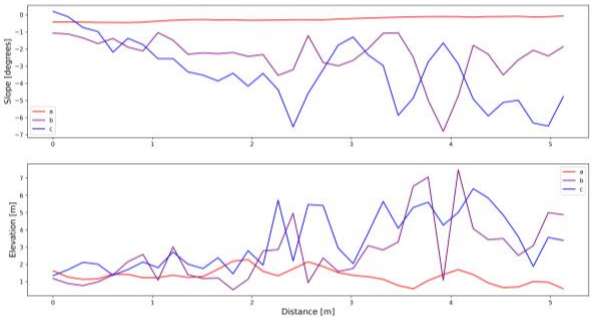

Figure 4. Topographic-profile analysis of ripples in Algodones Dunes. Inferred transport direction is left to right. Transect location shown in Figure 1.

Profile transects were drawn to analyze the length and orientation of the large and small wavelength ripples (Fig. 2). Transects were drawn perpendicular to the ripple crests and used to calculate average wavelengths.

Results and Discussion: The ripples are overall trending southwest-northeast with a large ripple orientation of 79.8° and a small ripple orientation of 77.81 (Fig. 3). The consistent orientations imply a dominant northwest-southeast wind direction that affects both bedforms similarly despite differences in wavelength (average large ripple wavelength is .39 m and small ripple wavelength is .13 m). Average length of the large and small ripples is .91 m, implying that the large ripples have a larger defect density compared to the small ripples which accounts for the similar length averages despite the scale difference.

Because of the very low relief of the coarse-grained ripples (~0.05 m), the DEM was detrended using Krieging so better visually examine the 3D nature of the coarse-grained ripples and to help confirm the visual crestline mapping that was undergone.

After analyzing profile curvature, tangential curvature, relief, slope, and visual layers, it was determined that the stoss slopes had a narrow slope azimuth mainly facing west-northwest while lee slopes largely faced east-northeast. The slope azimuth bins were reclassified. The stoss faces have a sum area of 845.49 m² while the lee faces have a sum area of 696.33 m². The stoss has an average slope of 10.80° while the lee face has an average slope of 8.23 degrees (Fig. 3). Low slope areas in Figure 3 shows the crests and troughs of the ripples and the highest slopes occur in the middle of the stoss slope. This is somewhat unexpected as lee slopes are typically steeper but may be a distinctive topographic feature of coarse-grained ripples or may be explained by bimodal winds that tend to flatten the ripples [3]. The slope is also likely affected by the underlying increasing elevation trend in the study area to the east.

Conclusion: This initial assessment of the topography of a coarse-grained ripple field shows that, as with dunes, their stoss and lee slopes can be well defined by their topographic structure, but the slope distributions across a ripple differ significantly from a dune. The lee slopes have overall lower slopes than the stoss and the maximum slopes occur in the middle of the stoss slope, which may be related to the feedbacks with the wind controlling the streamline curvature of the ripples [10]. Assessment of this entire field will increase the statistics of these slope distributions and allow an evaluation of the general nature of this characteristic.

The detailed topography created from low-altitude drone flights demonstrates the usefulness of such data for evaluating bedform patterns that are typically below the resolution of orbital data. As with dunes, now large data sets of 2D and 3D pattern parameters can be generated for ripples. Defining these characteristics on Earth provides a sound basis to evaluate ripples on Mars and other worlds and increases our ability to assess climate and environmental signals from these bedforms.

Acknowledgements: Part of this research has been supported by NASA SSW grant # 80NSSC20K0145

References: [1] Bagnold R. A. (1941) *The Physics of Blown Sand and Desert Dunes*. [2] Day M. and Kocurek G. (2018) *Geology*, *46*(11), 999-1002. [3] Derickson D. et al. (2008) *Geomorphology*, *99*(1), 186-204. [4] Ellwood J. M. et al. (2008) *Geomorphology*, *99*(1), 186-204.[5] Ewing R. C. et al. (2017) *JGR: Planets*, *122*(12), 2544-2573. [6] Ewing R. C. et al. (1975) *Journal of Sedimentary Research*, *45*(2), 554-561. [7] Jerolmack D. J. et al. (2006) *JGR Planets*, *111*(E12). [8] Lapotre M. G. A. et al. (2016) *Science*, *353*(6294), 55-58. [9] Sharp R.P.. (1963) *Wind Ripples*, 617-636.[10] Silvestro S. et al. (2020) *JGR Planets*, *125.8*. .[11] Sullivan R. et al. (2008) *JGR Planets*, *113*(E6).